Identification of the Fragmentation Role in the Amyloid Assembling Processes and Application to their Optimization

Monique Chyba* Jean-Michel Coron† Pierre Gabriel‡ Yuri Mileyko*
Human Rezaei§

Abstract

The goal is to establish a kinetic model of amyloid formation which will take into account the contribution of fragmentation to the de novo creation of templating interfaces. We propose a new, more comprehensive mathematical model which takes into account previously neglected phenomena potentially occurring during the templating and fragmentation processes. In particular, we try to capture a potential effect of the topology and geometry of prion folding on the elongation and fragmentation properties of a polymer of a given length by separating polymers of the same length into several compartments. Additionally, we apply techniques from geometric control to the new model to design optimal strategies for accelerating the current amplification protocols, such as the Protein Misfolding Cyclic Amplification (PMCA). The objective is to reduce the time needed to diagnose many neurodegenerative diseases. Determining the optimal strategy for accelerated replication in the general problem of fragmentation optimization is still an open question.

1 Introduction

Our goal is to investigate the contribution of the fragmentation process in the amyloid assembly formation and spreading. In a pathology caused by amyloid fibril formation, such as Prion, Alzheimer's, Parkinson's and other amyloidoses, the fragmentation of amyloid fibrils constitutes a unique pathway to spread the replication centre and propagate the pathology within tissues and between organs (Figure 1). Most of the kinetics models of protein polymerization in the literature implicitly include the fragmentation of polymers in the conversion process by assuming that the rate of fragmentation is negligible in comparison to the polymerization rate [11, 12, 19]. However, the real contribution of fragmentation to the polymerization enhancement as well as the molecular mechanisms of its occurrence remain unexplored. To establish for the first time a kinetic model

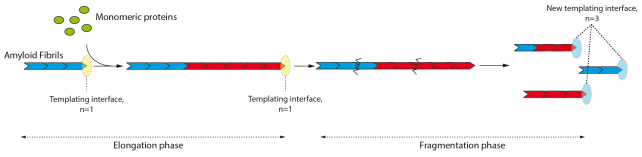

Figure 1: Templating and fragmentation processes lead to de novo generation of templating interfaces. The widespread theory for amyloid fibril spreading is based on the templating phenomenon, where the amyloid assembly which constitutes the template induces a structural change in the monomeric substrate. The templating process leads to an increase in the size of amyloid fibrils but keeps the number of templating interfaces constant. This phase corresponds to the elongation phase. Once a threshold size has been reached, the probability of the occurrence of fragmentation increases. The fragmentation phase leads to the generation of de novo templating interfaces.

of amyloid formation which will take into account the contribution of fragmentation to the de novo creation of templating interfaces, we need to combine mathematical modeling, theoretical and computational studies as well as experimental approaches. In this paper, we focus on a new model. In particular, we try to capture a potential effect of the topology and geometry of prion folding on the elongation and fragmentation properties of a polymer of a given length. Such an effect necessitates the assumption that polymers of the same length might fragment and elongate in different ways. Consequently, we separate polymers of the same length into several compartments.

An additional goal is to apply techniques from geometric control to the new model to design optimal strategies for accelerating the current amplification pro-

*Department of Mathematics, University of Hawaii at Manoa, 2565 McCarthy Mall, Honolulu, Hawaii 96822, USA. Email: chyba@hawaii.edu, yury@math.hawaii.edu

†Laboratoire Jacques-Louis Lions, UMR 7598, Universit Pierre et Marie Curie-Paris 6, 75005 Paris, France. E-mail: coron@ann.jussieu.fr

‡Université de Versailles Saint-Quentin-en-Yvelines, Laboratoire de Mathématiques de Versailles, CNRS UMR 8100, 45 Avenue des États-Unis, 78035 Versailles cedex, France. Email: pierre.gabriel@uvsq.fr

§National Institute for Agricultural Research (INRA), Pathological Macro-assemblies and Prion Pathology group (MAP2), UR892, Virologie Immunologie Molculaires, Jouy-en-Josas, 78350-F, France. E-mail: human.rezaei@jouy.inra.fr

tocols, such as the Protein Misfolding Cyclic Amplification (PMCA). The objective is to identify keys parameters controlling the spreading centre on amyloid fibrils elongation. We present here a preliminary analysis, but the long term expected results could be generalized to all neuropathologies caused by protein misassembly, such as Prion, Alzheimer's and Parkinson's diseases, which involve amyloid fibril formation.

2 Fibril fragmentation

Fibril fragmentation has been reported to enhance the polymerization process underlying the behavior of some specific prions. The mechanism of this enhancement is mainly based on the generation of supernuclei [10], which according to the Oosawa general model [14, 15] create a shortcut in polymerization. It has been proposed that the fragmentation process was at the origin of replication and propagation of pathogenic structural information of prions in general. According to this theory (which is largely accepted in the prion field and is being extended to other pathologies involving amyloid formations) a certain perturbation leads to a structural change in the native protein (unable to form an amyloid) thus creating a conformer prone to form amyloid assemblies. Once amyloid assemblies form, they serve as templates and convert the native protein into amyloidogenic in an apparently autocatalytic process.

Nonetheless, a number of unanswered questions remain concerning the experimental evidence of such an autocatalytic propagation. There are two physicochemical phenomena in the amyloidogenic process which cannot be ignored: the first one is the structural switch which triggers the formation of the first assembly; the second phenomenon is the fragmentation based amplification of the amyloidogenic process by the de novo generation of the templating interfaces (see Figure 1). The former phenomenon has been extensively explored, its molecular mechanisms are well understood, and several mathematical models have been developed. However, there is a significant lack of knowledge concerning the fragmentation process and the de novo generation of templating interfaces, both in the mechanisms of its occurrence and its contribution to the acceleration of the pathology.

We propose a first approach to study the behavior of this complex system by computer simulation. The computational model will allow us to simulate variations in the variables characterizing the system, and the results of the model simulation will guide the team of neuroscientists in their experiments.

3 Compartmental model of amyloid formation

The first stage of the computational model is to identify the size dependence of the fragmentation rate and the behavior of the generated fragments as: new templates; inert fragments and new monomers. We propose a new, more comprehensive mathematical model which takes into account previously neglected phenomena potentially occurring during the templating and fragmentation processes.

This compartmental approach is new. There is a lack of knowledge concerning the exchanges between the compartments, and further experimental study combined with computer simulations will play a crucial role in this aspect of the project.

A first attempt of optimizing the PMCA by using a mathematical model has been introduced in [7] and analyzed in [3, 5]. This prior model takes into account only the size dependence of the polymers, assuming that two polymers with the same length have exactly the same behavior. It also assumes that the monomers saturate the substrate, so that the polymerization and fragmentation intensities depend only on a control parameter which represents the action of the experimentalists on the dynamics of the system (by means of *sonication* in the case of the PMCA, see [7]). The resulting model writes as follows :

$$\dot{x}_i(t) = r(u(t))\big[\tau_{i-1}x_{i-1}(t) - \tau_i x_i(t)\big] + u(t)\Big[2\sum_{j=i+1}^{n}\beta_j\kappa_{ij}x_j(t) - \beta_i x_i(t)\Big]. \tag{3.1}$$

The unknown $x_i(t)$ represents the quantity of polymers with size $i \in \{1, \cdots, n\}$ at time t, τ_i is the transition rate from size i to $i+1$, β_i is the fragmentation rate for polymers of size i, and κ_{ij} is the probability for getting a polymer of size i from the fragmentation of a polymers of size $j > i$. The control $u(t)$ stands for the intensity of the sonicator. For any fixed control parameter $u \in \mathbb{R}_+^*$, model (3.1) is a linear system of differential equations with a corresponding matrix which is irreducible and has nonnegative off-diagonal entries. It is well known that such matrices possess a dominant Perron eigenvalue which prescribes the asymptotic exponential growth rate of the solutions. Consequently model (3.1) possesses for any fixed control $u \in [u_{\min}, u_{\max}]$ a Perron eigenvalue $\lambda_P(u)$ and it is proved in [5] that, for biologically relevant coefficients, the function $u \mapsto \lambda_P(u)$ can reach a maximum between $u_{\min}$ and $u_{\max}$. It has been emphasized in [2, 3, 5] that the value $u^* \in (u_{\min}, u_{\max})$ which maximizes λ_P plays a crucial role in the analysis of the singular arcs of the optimal control problem (see Section 4).

The main improvement in the new proposed model

is to take into account the variability between different polymers of the same size by dividing them into compartments. We denote by $x_i^l(t)$, $l = 1, \cdots, k_i$, the density of polymers of size i in compartment l at a given time t. The corresponding rate of change due to elongation is then described as follows:

$$r(u(t))\Big[\sum_{s=1}^{k_{i-1}} \tau_{i-1}^{l,s} x_{i-1}^s - \sum_{r=1}^{k_{i+1}} \tau_i^{r,l} x_i^l\Big]$$

where $\tau_{i-1}^{l,s}$ is the growth rate of polymers of size $i-1$ in compartment s that grow in compartment l of polymers of size i, and $\tau_i^{r,l}$ is the growth rate of polymers of size i in compartment l that grow into polymers of size $i+1$ (in compartment r). The fragmentation rate of change is expressed by the fact that polymers of a given size and given compartment fragment into polymers of a given size and compartment at different rates. More precisely, we have:

$$u(t)\Big[2\sum_{j=i+1}^{n}\sum_{s=1}^{k_j} \beta_j^s \kappa_{ij}^{l,s} x_j^s - \beta_i^l x_i^l\Big]$$

where β_i^l (β_i^s) represents the fragmentation coefficient of polymer of size i in compartment l (s) and the coefficient $\kappa_{ij}^{l,s}$ captures the fraction of polymer of size j that fragment from compartment s into size i polymer in compartment l. An illustration of some possible interactions between different compartments is shown in Figure 2. The experiments will determine the fragmentation rules between the compartments which will translate into relations among the parameters $\kappa_{ij}^{l,s}$. It is expected that there is a limitation on the polymers which can be fragmented into a given polymer, and therefore many of the $\kappa_{ij}^{l,s}$ will actually be zero. This is important to allow for an analysis of the system. It is also possible that the standard assumptions on $\kappa_{ij}^{r,s}$ will still hold:

$$\sum_{i=1}^{j-1}\sum_{r=1}^{k_i} \kappa_{ij}^{r,s} = 1, \quad \sum_{i=1}^{j-1} i \sum_{r=1}^{k_i} \kappa_{ij}^{r,s} = \frac{j}{2}.$$

To summarize, we propose a model of the form:

$$\begin{aligned}(3.2)\quad \dot{x}_i^l(t) = r(u(t))\Big[\sum_{s=1}^{k_{i-1}} \tau_{i-1}^{l,s} x_{i-1}^s(t) - \sum_{r=1}^{k_{i+1}} \tau_i^{r,l} x_i^l(t)\Big] \\ + u(t)\Big[2\sum_{j=i+1}^{n}\sum_{s=1}^{k_j} \beta_j^s \kappa_{ij}^{l,s} x_j^s(t) - \beta_i^l x_i^l(t)\Big].\end{aligned}$$

As in [5], equation (3.2) can be written in a matrix form:

$$\dot{x}(t) = (u(t)A + r(u(t))B)\, x(t)$$

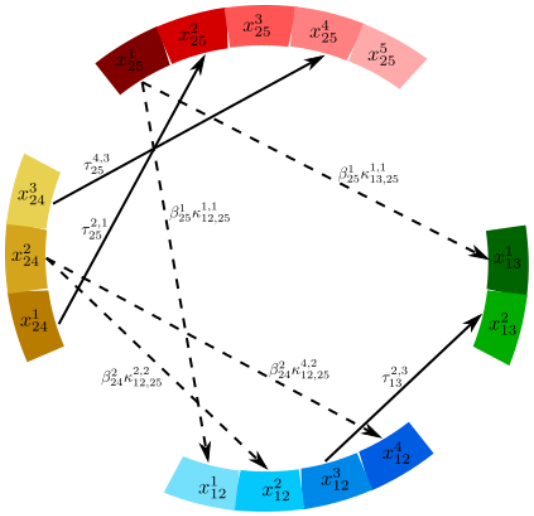

Figure 2: Possible interaction between different compartments of polymers of sizes $12, 13, 24, 25$. Solid arrows indicate growth, dashed arrows indicate fragmentation.

However, the growth matrix, B, and the fragmentation matrix, A, as well as vector $x(t)$, now have a block structure with blocks corresponding to the different compartments. More specifically, we have

$$x(t) = \begin{pmatrix} x_1(t) \\ \vdots \\ x_n(t) \end{pmatrix},\ A = \begin{pmatrix} 0 & & \\ & -A_1 & \begin{pmatrix} 2K_{ij} \end{pmatrix} \\ & 0 & \ddots \\ & & -A_n \end{pmatrix},$$

$$B = \begin{pmatrix} -D_1 & & & \\ T_1 & -D_2 & & 0 \\ & \ddots & \ddots & \\ & 0 & T_{n-2} & -D_{n-1} \\ & & & T_{n-1} \quad 0 \end{pmatrix},$$

where $x_i(t) = (x_i^1(t), \ldots, x_i^{k_i}(t))^\top$, $T_i = (\tau_i^{r,s})$ is a $k_{i+1} \times k_i$ matrix representing growth rates of polymers of size i, $D_i = \operatorname{diag}\left(\sum_{r=1}^{k_{i+1}} \tau_i^{r,s}\right)_{s=1}^{k_i}$, $A_i = \operatorname{diag}(\beta_i^s)_{s=1}^{k_i}$, and $K_{ij} = (\beta_j^s \kappa_{ij}^{r,s})$ is a $k_i \times k_j$ fragmentation matrix for polymers of size j.

If matricies A and B do not depend on x and t, then, similarly to model (3.1), model (3.2) is a linear system with a constant matrix which is irreducible and has non-negative off-diagonal entries. Hence, we can again pursue a model analysis based on the dominant Perron eigenvalue. It is then possible to show that there is an optimal value of the control, u^*, for which the Perron eigenvalue, $\lambda_P(u)$ attains its global maximum:

THEOREM 3.1. *Assume that $r : \mathbb{R}_+ \to \mathbb{R}_+$ is continu-*

ous and there exist $q > 0$ *and* $r_q \geq 0$ *such that*

$$r(u) = r_0 + r_q u^{-q} + o(u^{-q}), \text{ as } u \to +\infty$$

Then there exists u^* *such that* $\lambda_P(u) \leq \lambda_P(u^*)\ \forall u \geq 0$.

However, the growth rate matrix, B, may, in general, depend on time and/or polymer concentration, i.e. $B = B(t, x(t))$, thus making the above approach inapplicable. In such a case, we may need to employ to extensive computer simulations to obtain a better understanding about the system behavior.

As mentioned previously, the parameters will be determined experimentally. However, the complexity of the system and large number of parameters will require implementation of parameter estimation methodologies to help guide the experimentalists. In particular, using already available experimentally observable quantities, such as the distribution of polymer densities, we can employ standard Markov Chain Monte Carlo (MCMC) techniques to find regions of parameter values of high probability. These regions can then be narrowed by obtaining additional experimental data and running the estimation procedure starting with the previously obtained estimate.

Once the compartments and the communication between them is well identified, the behavior inside each compartment also needs to be determined. In particular the in vitro elongation of the fibrils appears to saturate after some time and the polymerization process is then blocked. This saturation effect has to be understood and included in the model. It requires us to identify which compartments are mainly responsible for the saturation. We propose to investigate two possible explanations of the saturation effect: it is caused either by the monomers, or by inert polymers. The monomers could be responsible for the saturation because they may be not in a sufficient quantity in the substrate (not saturating), or only a portion of them could be transconformed, and once they are consumed the reaction stops. Alternatively, there can be polymers which are not all able to attach monomers, or which loose this ability after some time or when they become too large. This would lead us to consider a compartment which empties with time and/or a "dead" compartment which behaves like a trash receptacle. In the model, this translates into $\tau_{i-1}^{l,s} \to 0$ as the size i gets bigger. If we assume that propensity to attach is more related to the age of the polymer and reduces with time, we can incorporate this into the model by making elongation parameters depend on time and have $\tau_{i-1}^{l,s}(t) \to 0$ as the duration of the experiment progresses. The model provides a lot of flexibility. We can also consider the assumption that the saturation effect is linked to a high density of polymers in the solution by introducing a production of monomers into the model and making the coefficients $\tau_{i-1}^{l,s}$ depend not only on time but also on the total concentration of polymers. Computer simulations of different versions of the model will expedite our research and help the experimentalists identify the actual physical experiments which have to be conducted. The model will be validated through an interplay between computer simulations and experimental observations. With the introduction of the compartments and the saturation effect into the new model of the fragmentation process (3.2), the solutions will behave very differently from the ones for the model given by (3.1). In particular, no exponential growth of the total population of polymers is expected. Computer simulations will provide insights into the qualitative and quantitative properties of the solutions to help guide the theoretical analysis. The fact that the function r in (3.2) is a decreasing convex function will be checked experimentally, and adapted if it is necessary. After adding the saturation effect the model becomes nonlinear, which raises new challenging mathematical questions. The preliminary work on the linear version in [2, 3, 5] is a solid base on which we can rely to address this new nonlinear problem.

4 Optimization of amplification protocols

Since incubation of a disease triggered by prions can take place over very long period of time, an important question is the optimization of the templating, elongation, and polymerization processes to accelerate the detection of the protein in an affected person. It is particularly relevant to PMCA, which is a technique to simulate an accelerated replication process for prions in a laboratory environment [18] by creating a cyclic scheme that alternates incubation phases to allow lengthening of the abnormal prion with sonication phases to break the polymers into smaller ones. Typically, [17], during the PMCA the incubation phase (no sonication) is more than 30 times the duration of the sonication phase (at a constant frequency) and alteration of these two phases takes place over 48 hours. This correspond to a bang-bang strategy with the control (sonication intensity) switching a finite number of times between its minimum and maximum values. Since the introduction of the PMCA scientists have tried to improve the protocol in various way [6, 8, 13], but there is no literature on the role that singular arcs could play to design a more efficient sonication scheme beside a first approach with the non compartmental model [3, 5]. We introduce here the tools necessary to analyse the singular arcs for the new model.

4.1 Mayer Problem From Section 3, the general expression for our system is of the form:

$$\dot{x}(t) = [Au(t) + B(t, x(t))r(u(t))]x(t), \tag{4.3}$$

$$x(0) = x_0 > 0, \tag{4.4}$$

where $x = (x_1^1, \cdots, x_1^{k_1}, \cdots, x_n^1, \cdots, x_n^{k_n}) \in R^m$, $m = \sum_{i=1}^n k_i$. Notice that the matrix A is constant since we assume that the fragmentation coefficients stay constant throughout the protocol. However, the elongation coefficients might various with time to reflect the saturation hypothesis. This implies that the matrix B is not constant but can depend explicitly on t or on the current density of polymers $x(t)$.

The quantity we would like to minimize is the final density of polymers and is expressed as $c(x(T)) = \sum_{i=1}^n (i \sum_{j=1}^{k_i} x_i^j(T))$. As in [5], we make here the assumption that the function r in (3.2) is a decreasing convex function. This will be checked experimentally, and adapted if it is necessary in further work. The functions f_0 and f_1 depend on the time and possibly the density of polymers to reflect the saturation phenomenon observed experimentally. The dependence is unclear at this stage and will be determined in further work. We introduce the following notations:

$$\Omega := \{(u, r(u));\ u_{\min} \leq u \leq u_{\max}\}, \tag{4.5}$$

$$\psi := (\psi_{k_1}, \cdots, \psi_{k_n}) \in R^m \tag{4.6}$$

where $\psi_{k_i} = (i, \cdots, i) \in R^{k_1}$ and ψ is called the mass vector.

The optimal control problem is $\max_u c(x(T))$ with a fixed $T > 0$, subject to $\dot{x} = [Au(t) + B(t, x(t))r(u(t))]x(t)$ with u a measurable bounded function such that $(u(t), r(u(t))) \in \text{Hull}(\Omega)$ for almost every $t \in [0, T]$, where $\text{Hull}(\Omega)$ is introduced to guarantee the existence of an optimal control. Under similar assumptions on the parameters $\tau_i^{s,l}, \beta_i^l, \kappa_{ij}^{s,l}$ than in [5] we can prove that the optimal control must belong to the line Σ defined by

$$\Sigma = \{(u, au + b);\ u_{\min} \leq u \leq u_{\max}\} \tag{4.7}$$

where $a = \frac{r(u_{\max}) - r(u_{\min})}{u_{\max} - u_{\min}}$ and $b = \frac{u_{\max} r(u_{\min}) - u_{\min} r(u_{\max})}{u_{\max} - u_{\min}}$. Using a reparametrization (to normalize $b = 1$), we can therefore rewrite the optimal problem as an affine single-input system:

$$\dot{x}(t) = f_0(t, x(t)) + f_1(t, x(t))u(t), \tag{4.8}$$

$$x(0) = x_0 > 0, \tag{4.9}$$

$$\min_{u_{\min} \leq u \leq u_{\max}} -\psi x(T), \tag{4.10}$$

where $f_0(t, x(t)) = B(t, x(t))$ and $f_1(t, x(t)) = Ax(t) + aB(t, x(t))$, $a < 0$. Our optimal control problem is in Mayer form with fixed time T but not constraints on the terminal state $x(T)$.

4.2 Necessary Conditions The maximum principle, see [1, 16], provides necessary conditions as a basis to compute optimal controls. For a Mayer problem the theorem below is a classical result.

THEOREM 4.1. *Consider the Mayer problem (4.8-4.10), and let $u^*(.)$ be an optimal control whose corresponding trajectory $x^*(.)$ is optimal. We introduce the pseudo-Hamiltonian $H(t, x, p, u) = \langle p, f_0(t, x)\rangle + \langle p, f_1(t, x)\rangle u$. Then, there exists an adjoint vector $p^*(.)$ such that for almost every $t \in [0, T]$,*

$$\dot{x}^* = \frac{\partial H}{\partial p}(t, x^*, p^*, u^*), \quad \dot{p}^* = -\frac{\partial H}{\partial x}(t, x^*, p^*, u^*)$$

$$H(t, x^*, p^*, u^*) = \max_{u \in [u_{\min}, u_{\max}]} H(t, x^*, p^*, u)$$

$$p^*(T) = \psi \ \text{(Transversality condition)}$$

A triple (x, p, u) solution of Theorem 4.1 is called an extremal. The maximization condition implies that along an extremal (x^*, p^*, u) we have

$$\langle p^*(t), f_0(t, x^*(t))\rangle + \langle p^*(t), f_1(t, x^*(t))\rangle u^*(t) =$$
$$\max_u \langle p^*(t), f_0(t, x^*(t))\rangle + \langle p^*(t), f_1(t, x^*(t))\rangle u$$

Since $\langle p^*(t), f_0(t, x^*(t))\rangle$ does not depend on the control it follows that $u^*(t)$ must be chosen such that it maximizes the function $\langle p^*(t), f_1(t, x^*(t))\rangle u$. By assumption we have $u_{\min} < u < u_{\max}$, therefore when the expression $\langle p^*(t), f_1(t, x^*(t))\rangle$ is negative u must be as small as possible and it must be the largest when $\langle p^*(t), f_1(t, x^*(t))\rangle > 0$. To summarize, since it is an affine single-input system, the maximization condition implies that along an extremal

$$u(t) = \begin{cases} u_{\min}\phi(t) \text{ if } \phi(t) < 0 \\ u_{\max}\phi(t) \text{ if } \phi(t) > 0 \end{cases} \tag{4.11}$$

where $\phi(t) = \langle p(t), f_1(t, x(t))\rangle$ is the so-called switching function. An extremal arc along which $\phi(t) \equiv 0$ is said to be singular, and regular otherwise. The maximum principle implies that an optimal solution $x^*(.)$ is the projection of a concatenation of bang and singular extremals, and the main difficulty is to analyze the structure of the optimal control.

4.3 Singular Arcs Singular arcs often play a major role in the optimal synthesis, see [1] and therefore need to be analyzed in details. To derive the calculations for a singular extremal we can assume the system to be autonomous. Indeed, in case we assume the coefficients to be time dependent (which would correspond to the case when some of the elongation parameters tend to zero after a given time) we introduce an additional state variable $\dot{x}_{m+1}(t) = 1$, $x_{m+1}(0) = 0$

and replace $f(t,x(t),u(t))$ by $f(x_{m+1}(t),x(t),u(t))$ to create an autonomous system with $f(\mathbf{x}(t),u(t))$ where $\mathbf{x}=(x_{m+1},x)\in R^{m+1}$.

We introduce $H_0(x,p)=\langle p,f_0(x)\rangle$ and $H_1(x,p)=\langle p,f_1(x)\rangle$ the respective Hamiltonian lifts. The maximization condition in the singular case is given by

$$H_1(x,p)\equiv 0. \tag{4.12}$$

Differentiating twice this equation we obtain

$$\{H_1,H_0\}(x,p)=0$$
$$\{\{H_1,H_0\}H_0\}(x,p)+u\{H_1,H_0\},H_1\}(x,p)=0$$

along the singular arc, where $\{H_X,H_Y\}(x,p)=H_{[X,Y]}(x,p)$ denotes the Poisson brackets for two vector fields X,Y using the convention $[X,Y](x)=\frac{\partial X}{\partial x}(x)Y(x)-\frac{\partial Y}{\partial x}(x)X(x)$. We obtain that outside the surface $S=\{(x,p);\ \{\{H_1,H_0\},H_1\}(x,p)=0\}$, the singular control is given by

$$u_s=-\frac{\{\{H_1,H_0\},H_0\}(x,p)}{\{\{H_1,H_0\},H_1\}(x,p)} \tag{4.13}$$

Lemma 4.1. *The generalized Legendre Clebsh condition* $\frac{\partial}{\partial u}\frac{d^2}{dt^2}\frac{\partial H}{\partial u}\leq 0$ *must hold along an optimal singular arc. For a single-input affine system like here it is equivalent to* $\frac{\partial}{\partial u}\ddot{\phi}\leq 0$. *In our case it is expressed as*

$$\{H_1,\{H_1,H_0\}\}(x,p)\leq 0. \tag{4.14}$$

In the autonomous case, which is equivalent in our problem to assume that the saturation phenomenon is triggered due to an over-population of polymers only and therefore the coefficients $\tau_{i-1}^{s,l}$ depend solely on x and not explicitly on t, we have the following. Since $f_0(x)=B(x),f_1(x)=Ax+aB(x)$ the expression $\{H_1,H_0\}(x,p)=\langle p,[f_1(x),f_0(x)]\rangle=\langle p,[Ax+aB(x),B(x)]\rangle$ which is equivalent to $\langle p,[Ax,B(x)]\rangle$ using the fact that $[B(x),B(x)]=0$. Similar calculations show that $\{\{H_1,H_0\},H_0\}(x,p)=\langle p,[[Ax,B(x)],B(x)]\rangle$ and $\{\{H_1,H_0\},H_1\}(x,p)=\langle p,[[Ax,B(x)],Ax+aB(x)]\rangle$. We obtained that the conditions for singular arcs are equivalent to

$$u_s=-\frac{\langle p,[[Ax,B(x)],B(x)]\rangle}{\langle p,[[Ax,B(x)],Ax]+a[[Ax,B(x)],B(x)]\rangle},$$

with

$$\langle p,[Ax,[Ax,B(x)]]+a[B(x),[Ax,B(x)]]\rangle\leq 0$$

and the following proposition holds.

Proposition 4.1. *Singular trajectories of order 1 are the projections* $x(t)$ *of extremals solutions of* $\dot{z}(t)=Z_s(z(t))$, $z=(x,p)$ *where* Z_s *is given by:*

$$Z(z(t))=\begin{pmatrix} B(x)+(Ax+aB(x))u_s(z)\\ \langle p,B'(x)+u_s(z)(A+aB'(x))\rangle\end{pmatrix} \tag{4.15}$$

where $u_s(z)$ *is given above.*

If at the contrary we assume that the saturation is solely a process due to the aging of the prions, then we have in system (4.8) that $f_0(t,x(t))=B(t)x(t)$ and $f_1(t,x(t))=Ax(t)+aB(t)x(t)$. It is now a non autonomous system and we break the bi-linearity of the system depending on the dependence of the parameters with respect to the time. By introducing $\mathbf{x}=(x_{m+1},x)$ and $\mathbf{p}=(p_{m+1},p)$, the augmented Hamiltonian becomes $H(\mathbf{x},\mathbf{p},u)=\langle p,B(x_{m+1})x\rangle+p_{m+1}+u\langle p,Ax+aB(x_{m+1})x\rangle$. The maximization condition implies that along a singular extremal we have

$$\langle p,Ax+aB(t)x\rangle\equiv 0 \tag{4.16}$$

where $t=x_{m+1}$. This expression is similar to the autonomous case, the difference is the term $B(t)$ that is now dependent on time. Differentiating this equation leads to one additional term beside the Lie bracket due to the time dependence of B, this term takes the form $\langle p,a\frac{dB}{dt}x\rangle$. We have the following result

$$\langle p,[Ax,B(t)x]+a\frac{dB}{dt}(t)x\rangle\equiv 0 \tag{4.17}$$

where $[A,B(t)]$ is computed in the m-dimensional space $x_1,\cdots,x_m$) and treating t as a constant. It is really easier to express the results in the m-dimensional space since the non autonomy is only related to part of the model (the time dependence of the parameters that only appear in the matrix B). To obtain the singular control we must differentiate once more this equation, clearly second order derivatives of $B(t)$ will appear. Straightforward computations show that

$$u_s(t)=-\frac{\langle p,D(x,t)\rangle}{\langle p,D'(x,t)\rangle} \tag{4.18}$$

where

$$D(x,t)=[[Ax,B(t)x],B(t)x]+[\frac{dB}{dt}(t)x,B(t)x]+[Ax,\frac{dB}{dt}(t)x]+a\frac{d^2B}{dt^2}(t)x,$$

and

$$D'(x,t)=[[Ax,B(t)x],Ax]+a[[Ax,B(t)x],B(t)x]+a[\frac{dB}{dt}(t)x,Ax]+a^2[\frac{dB}{dt}(t),B(t)].$$

Notice that many of those terms will simplify once we have an expression for the coefficients of the elongation process as a function of time.

4.4 Further work on singular arcs Based on the calculations above, the research program for the optimization protocol is now twofold. First, using geometric arguments (see [3, 5] for the case of the non-compartmental linear model) we need to further characterize the singular flow from the expression u_s obtained through the differentiation of the maximization condition. Moreover, to gain insights, the geometric classification of the singular flow in low dimensions should be conducted using Gröbner bases to analyze the singularities of the so-called singular surface. Second, a numerical investigation needs to be used to determine the optimal strategy. Two approaches are possible, one is called a direct method and transforms the infinite dimensional optimal control problem into a finite dimensional optimization problem and the other one is an indirect method based on the geometric analysis conducted with the maximum principle. It combines multiple shooting, differential continuation (or homotopy) methods and computation of the solutions of the variational equations, needed to check second order conditions of local optimality. Most likely, an hybrid strategy between the direct and indirect method will provide the best results. The respective softwares, open sources toolbox for optimal control problems, are called BOCOP (http://bocop.saclay.inria.fr/) and Hampath (http://cots.perso.math.cnrs.fr/hampath/). When using indirect method, a particular attention will be given to determining the conjugate points along the singular arcs, since the absence of conjugate points on each singular arc of a candidate solution is a necessary condition for local optimality. It was shown that for the preliminary model (3.1) the calculations of conjugate points were inconclusive, which was clearly a result of a nonrealistic model of the fragmentation process without the saturation phenomenon. Finally, a typical feature of optimal solvers is the existence of many locally optimal solutions calculated either by the direct or indirect method mentioned above. It is then vital to determine global optimality. A possibility to explore this issue is the use of moment/linear matrix inequality (LMI) technique and the toolbox GloptiPoly [9]. This research program presented above is intricate and out of the scope of this paper, it is a forthcoming study to be combined with data from experimental work to provide information on the parameters of the new model.

5 Acknowledgments

M. Chyba is partially supported by the National Science Foundation (NSF) Division of Mathematical Sciences, award #1109937. J.-M. Coron is partially supported by ERC advanced grant 266907 (CPDENL) of the 7th Research Framework Programme (FP7). P. Gabriel is partially supported by the project ANR-13-BS01-0004 (KIBORD) funded by the French Ministry of Research.

References

[1] M. Bonnard and M. Chyba, *Singular trajectories and their role in control theory*, Springer-Verlag, Berlin, 2003.

[2] V. Calvez, P. Gabriel, and S. Gaubert, *Non-linear eigenvalue problems arising from growth maximization of positive linear dynamical systems*, Proceedings of IEEE 53rd Annual Conference on Decision and Control (CDC 2014), Los Angeles, pp. 1600–1607.

[3] M. Chyba, J.-M. Coron, P. Gabriel, A. Jacquemard, G. Patterson, G. Picot, and P. Shang, *Optimal geometric control applied to the protein misfolding cyclic amplification process*, Acta Appl. Math., in press (2015), DOI 10.1007/s10440-014-9950-8.

[4] M. Chyba, G. Patterson, G. Picot, *et al.*, *Designing rendezvous missions with mini-moons using geometric optimal control*, J. Ind. Manag. Optim., 10 (2014), pp. 477–501.

[5] J.-M. Coron, P. Gabriel, and P. Shang, *Optimization of an amplification protocol for misfolded proteins by using relaxed control*, J. Math. Biol., 70 (2015), pp. 289–327.

[6] N. Fernández-Borges and J. Castilla, *PMCA. A decade of in vitro prion replication*, Current Chem. Biol., 4(2010), pp. 200–207.

[7] P. Gabriel, *Équations de transport-fragmentation et applications aux maladies à prions*, PhD thesis, Université Pierre et Marie Curie-Paris VI, 2011.

[8] N. Gonzalez-Montalban, N. Makarava, V. G. Ostapchenko, *et al.*, *Highly efficient protein misfolding cyclic amplification*, PLoS Pathog., 7(2009), e1001277.

[9] D. Henrion, J. B. Lasserre, and J. Lofberg, *Gloptipoly 3: Moments, optimization and semidefinite programming*, Optim. Methods Software, 4 (2009), pp. 761–779.

[10] D. Kashchiev, *Nucleation*, Butterworth-Heinemann, 2000.

[11] T. P.J. Knowles, C. A. Waudby, G. L. Devlin, S. I.A. Cohen, A. Aguzzi, M. Vendruscolo, E. M. Terentjev, M. E. Welland, and C. M. Dobson, *An analytical solution to the kinetics of breakable filament assembly*, Science, 326 (2009), pp. 1533–1537.

[12] J. Masel, V. A.A. Jansen, and M. A. Nowak, *Quantifying the kinetic parameters of prion replication*, Biophys. Chem., 77 (1999), pp. 139–152.

[13] C. E. Mays, W. Titlow, T. Seward, *et al.*, *Enhancement of protein misfolding cyclic amplification by using concentrated cellular prion protein source*, Biochem. Biophys. Research Comm., 388 (2009), pp. 306–310.

[14] F. Oosawa and S. Asakura, *Thermodynamics of the Polymerization of Protein*, Academic Press, 1975.

[15] F. Oosawa and M. Kasai, *A theory of linear and helical aggregations of macromolecules*, J. Mol. Biol., 4 (1962), pp. 10–21.

[16] L. S. Pontryagin, V. G. Boltyanskii, R. V. Gamkrelidze, *et al.*, *The Mathematical Theory of Optimal Processes*, John Wiley & Sons, New York, 1962.

[17] P. Saa and J. Castilla and C. Soto, *Ultra-efficient Replication of Infectious Prions by Automated Protein Misfolding Cyclic Amplification*, Biological Chemistry 281(16)(2006), pp. 35245- 3525.

[18] G. P. Saborio, B. Permanne, and C. Soto, *Sensitive detection of pathological prion protein by cyclic amplification of protein misfolding*, Nature, 411(2001), pp. 810–813.

[19] W.-F. Xue, S. W. Homans, and S. E. Radford, *Systematic analysis of nucleation-dependent polymerization reveals new insights into the mechanism of amyloid self-assembly*, Proc. Natl. Acad. Sci., 105 (2008), pp. 8926–8931.